Korean J. Chem. Eng., **24**(6), 1084-1088 (2007)

Growth of ZnO nanoneedles on silicon substrate by cyclic feeding chemical vapor deposition: Structural and optical properties

Suk Lee, Ahmad Umar, Sang Hoon Kim, N. Koteeswara Reddy and Yoon-Bong Hahn†

School of Semiconductor and Chemical Engineering, and Nanomaterials Processing Research Centre,
Chonbuk National University, Jeonju 561-756, Korea
(*Received 14 July 2006 • accepted 10 March 2007*)

Abstract−Well-crystallized ZnO nanoneedles were grown on Au-coated Si(100) substrate by cyclic feeding chemical vapor deposition (CFCVD) process using diethyl zinc and oxygen as precursors for zinc and oxygen, respectively. Morphological investigations revealed that the as-grown nanoneedles exhibited sharpened tips and wider bases, having the typical diameters at their bases and tips, 60±10 nm and 20±10 nm, respectively. Detailed structural characterizations confirmed that the as-grown products were single crystalline with a wurtzite hexagonal phase and were grown preferentially along the [0001] direction. The room-temperature photoluminescence (PL) spectrum showed a strong and sharp UV emission at 378 nm with a very weak, suppressed and broad green emission at 520 nm, substantiating good optical properties for the as-grown ZnO nanoneedles.

Key words: ZnO, Nanoneedles, Cyclic Feeding Chemical Vapor Deposition, Optical Properties

INTRODUCTION

After the discovery of carbon nanotubes by Iijima in 1991 [1], the one-dimensional nanostructures, such as nanowires, nanorods, nanoneedles, nanobelts, nanotubes etc., have attracted considerable attention for their exceptional, unique and excellent electronic, electrical, optical and mechanical properties and their potential uses in both fundamental and practical studies. Heretofore, the synthesis and applications of various semiconductors one-dimensional nanostructures were reported in the literature, for instance GaN, ZnSe, SiC, Si, ZnO, SnO_2 etc. [2-8], but among all types of semiconducting one-dimensional nanostructures, the II-VI wurtzite hexagonal ZnO has a special place due to its exotic properties and wide uses in both fundamental scientific research as well as their potential applications for the fabrication of efficient nanodevices [7-21]. Due to its wide band gap (3.37 eV) and higher exciton binding energy (60 meV), which is much larger than other semiconductor materials such as GaN (25 meV) and ZnSe (22 meV), it presents itself as an important and promising material for UV photonic devices [9], sensors, piezoelectric and optical devices, etc. [10]. Because of its wide applications, the ZnO nanomaterials are the subject of extensive research nowadays. Hitherto, various kinds of ZnO nanostructures such as nanowires [5], nanorods [7,8], nanotubes [11], nanobelts [12], nanobows [13], nanorings [14], nanosprings [15], nanostars [6], nanoflowers [16], nanosheets networks and nanodisks [17], nanocolumns [18] nanoneedles [19-23] etc., have been fabricated by different fabrication techniques and reported in the literature. Among these different types of ZnO nanostructures, the ZnO nanoneedles are gaining particular interest because of their sharp curvature at their tips, which provides for many applications for the fabrication of various devices, such as field emission devices (FEDs), probing tips with high spatial resolution in vertical as well as horizontal diameter and atomic force microscopy tips [24] etc.

In this paper, we report the synthesis of ZnO nanoneedles by a cyclic feeding chemical vapor deposition (CFCVD) technique, which had been first used in our previous works to grow star-shaped and flower-shaped ZnO nanostructures [6,16]. The CFCVD system is based on the cyclic feeding of reactant precursors, where each precursor is introduced into the reaction chamber after a certain time interval and thus no reaction occurs in the gas phase. Unlike the conventional ALD system, our approach produced one-dimensional nanostructures on substrates instead of thin films. Moreover, CFCVD provides low impurity content in the deposited nanostructures. In addition to this, the deposition temperature to fabricate the nanostructures by CFCVD is lower than other fabrication methods. The as-grown nanoneedles were characterized in terms of their structural and optical properties, and finally a plausible growth process has been proposed for the formation of ZnO nanoneedles.

EXPERIMENTAL SECTION

ZnO nanoneedles were grown by the cyclic feeding chemical vapor deposition (CFCVD) system. Details of the CFCVD system are reported elsewhere [6]. A 1.5×1.5 cm sized 10 nm Au coated Si(100) substrate was used as a substrate for this synthesis. The Au was deposited on the Si(100) substrate by the electron beam evaporation technique. Commercially available diethyl zinc (DEZn) and high purity oxygen (99.999%) gas were used as precursors of Zn and oxygen, respectively, while argon was used as a carrier and purging gas during the reaction. The diethyl zinc (DEZn) bubbler temperature was kept constant at 5 °C during the whole reaction process. During the synthesis, one deposition cycle for the ZnO nanoneedles was completed in 31 s with four consecutive pulses. Between the 2 s pulse of DEZn and 5 s pulse of O_2, a 12 s pulse of argon gas was introduced into the reaction chamber. This opening and closing pulses of the reactants were controlled by the computer. During the deposition process the substrate temperature was in the range

†To whom correspondence should be addressed.
E-mail: ybhahn@chonbuk.ac.kr

of 400-475 °C. After the reaction was completed a gray colored film was deposited onto the Au coated Si(100) substrate which was characterized with respect to its structural and optical properties.

The general morphologies and detailed structural properties of the as-grown ZnO nanoneedles were characterized by field emission scanning electron microscopy (FESEM) and high resolution transmission electron microscopy (HRTEM) equipped with a selected area electron diffraction (SAED) pattern, respectively. The chemical compositions and crystal structures of the as-grown products were observed by using the energy dispersive X-ray (EDX) spectrometry and X-ray diffraction (XRD) pattern with Cu-Kα radiations, respectively. The room-temperature photoluminescence (PL) measured by using the He-Cd laser line with an excitation source of 325 nm was used to characterize the optical properties of the as-grown ZnO nanoneedles.

RESULTS AND DISCUSSIONS

1. Detailed Structural Characterization of ZnO Nanoneedles

Fig. 1(a) and 1(b) show the low and high magnification FESEM images of the ZnO nanostructures grown onto the Au-coated Si(100) substrate by the CFCVD at 400-475 °C. The microscopic observations indicate that the deposited nanostructures are needle-shaped and are grown onto the substrate surface in a high density. The obtained ZnO nanoneedles exhibit sharpened tips with wider bases

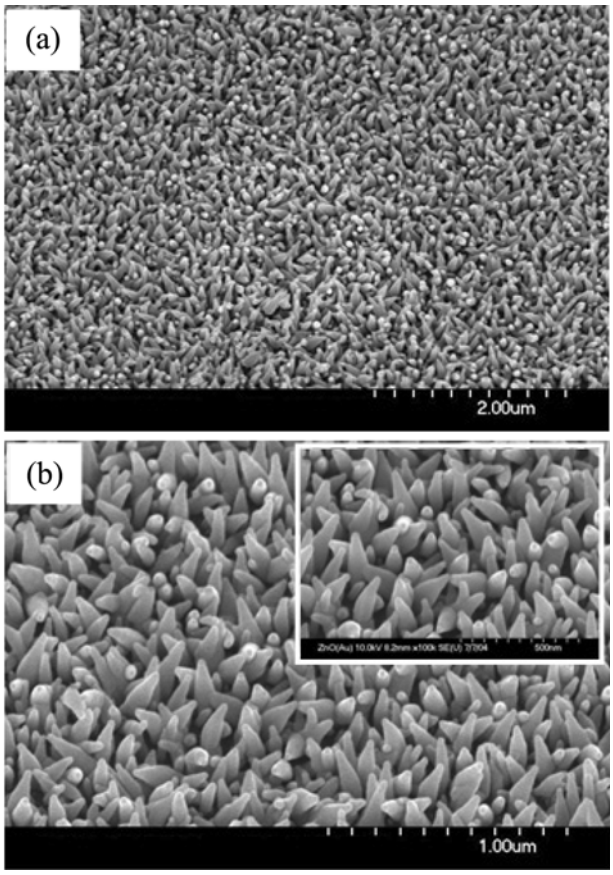

Fig. 1. FESEM images of ZnO nanoneedles grown on Au-coated Si(100) substrate by the cyclic feeding chemical vapor deposition: (a) low and (b) high magnification images.

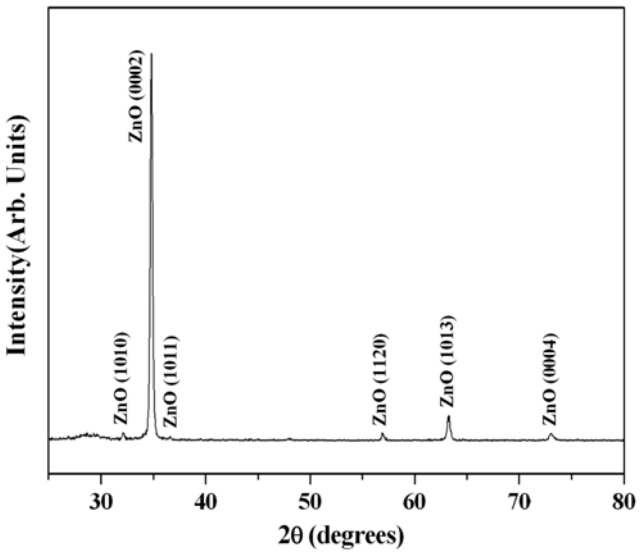

Fig. 2. X-ray diffraction pattern of ZnO nanoneedles grown on Au-coated Si(100) substrate: indexed peaks are corresponds to the wurtzite hexagonal phase for grown nanostructures.

and are partially aligned to the substrate surface. The lengths of the grown nanostructures are varying from each other from 250 nm to 350 nm. The nanoneedles show small length as compared to other reported ZnO nanoneedles, which were grown via the thermal evaporation or metal organic chemical vapor deposition (MOCVD) process. The short length of the nanoneedles in our case was due to a smaller number of deposition cycles (75-100 cycles). Moreover, it is important to note that the needle-shaped ZnO nanostructures by CFCVD are reported for the first time in this paper. The diameters of the needle-shaped ZnO nanostructures varied from the top to the bottom. The typical diameters at their bases and tips are 60±10 nm and 20±10 nm, respectively.

The crystallinity and crystal phase of the deposited ZnO nanoneedles were examined by the X-ray diffraction (XRD) patterns with Cu-Kα radiation and depicted in Fig. 2. All the indexed peaks in the spectrum are well matched with the X-ray diffraction pattern for the bulk single-crystalline ZnO (JCPDS Card No. 36-1451), which confirms that the synthesized products are single crystalline ZnO and possess a wurtzite hexagonal phase. No other peaks related to impurities were detected from the spectrum within the detection limit of the X-ray diffraction, further confirming that the obtained products are pure ZnO. Moreover, a strong intensity and highest peak in the spectrum at 34.2°, corresponding to [0002], indicated that the as-grown nanostructures are preferentially oriented in the c-axis direction. The higher intensity and narrower spectral width of the [0002] peak as compared to other ZnO peaks like [1010] and [1011] indicated that the as-grown ZnO nanoneedles are highly crystalline with a wurtzite hexagonal phase and grown along the [0001] direction. The chemical compositions of the deposited products were determined by the EDX measurement and shown in Fig. 3, which reveals that the as-grown ZnO nanoneedles are composed of Zn and oxygen only. Additionally, the atomic ratios of Zn : O fits almost 1 : 1 stoichiometry of Zn and oxygen, respectively. The silicon and carbon signatures are from silicon substrate and carbon film coated onto the FE-SEM grid, respectively. Detailed structural character-

ization of the grown ZnO nanoneedles was performed by transmission electron microscopy (TEM) combined with the selected area electron diffraction (SAED) patterns.

Fig. 4(a) shows the low magnification TEM images of ZnO nanoneedles, which is fully consistent with the FESEM observations and reveals that the as-grown nanostructures have sharpened tips and wider bases. The diameters of the basal portion of nanoneedles varied from the tip portion and lie in range of 50-70 nm and 10-30 nm, respectively. Fig. 4(b) shows the high-resolution TEM (HRTEM) image of the grown ZnO nanoneedles, which indicates that the synthesized products are single-crystalline and grown along the [0001] direction. The distance between two lattice fringes of the grown nanostructures is 0.52 nm, equal to the lattice constant of ZnO, which further confirms the single-crystallinity and wurtzite hexagonal phase for the synthesized nanoneedles. The corresponding SAED pattern of the as-grown nanoneedles is consistent with the HRTEM observations and indicated the single crystallinity and c-axis growth direction for the grown nanostructures (inset (b)). Interestingly, it was observed that some of the nanoneedles were exhibiting scratch lines on their outer surfaces. After a detailed examination by HRTEM of these scratch lines, it was found that these originated due to the improper formation or mismatch of ZnO stacks during deposition and called as "stacking faults" (Fig. 4(b)). Gerthsen et al. have reported that the stacking faults in the nanostructures were created by the condensation of interstitial Zn atoms and besides, interstitial Zn atoms can induce the formation of oxygen vacancies [25].

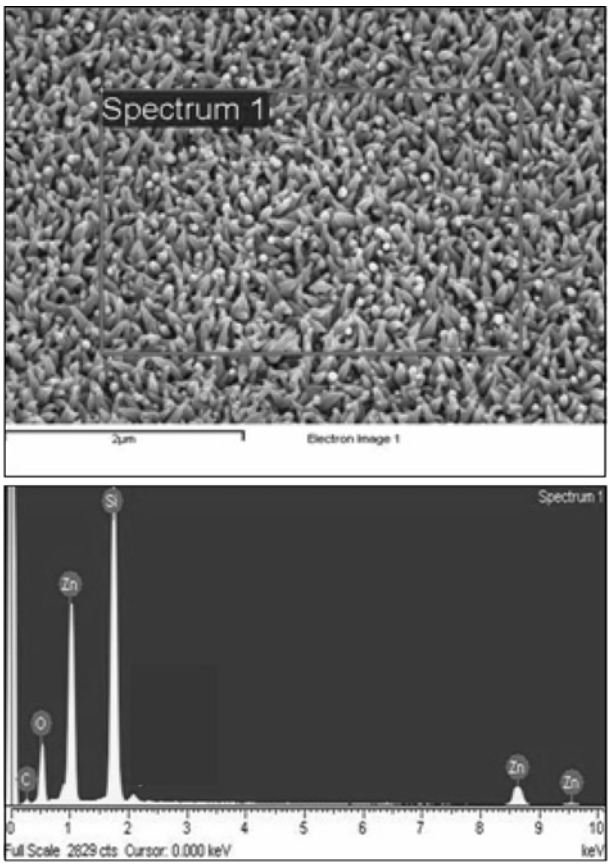

Fig. 3. Energy dispersive X-ray (EDX) spectroscopy of ZnO nanoneedles grown on Au-coated Si(100) substrate.

2. The Photoluminescence (PL) Properties of ZnO Nanoneedles

The optical properties of as-grown ZnO nanoneedles were examined by photoluminescence (PL) measurements at room temperature by using an He-Cd laser-line with an excitation wavelength of 325 nm, and shown in Fig. 5. Two bands have appeared in the PL spectrum, i.e., in UV and visible regions. A strong, sharp and dominating band at 378 nm in the UV region and a weak and suppressed band at 520 nm in the visible regions have been observed. The UV emission is also called the near band edge emission which originated due to the free-exciton recombination while the green emission known to be as deep level emission was generated by the impurities and structural defects such as oxygen vacancies and Zn

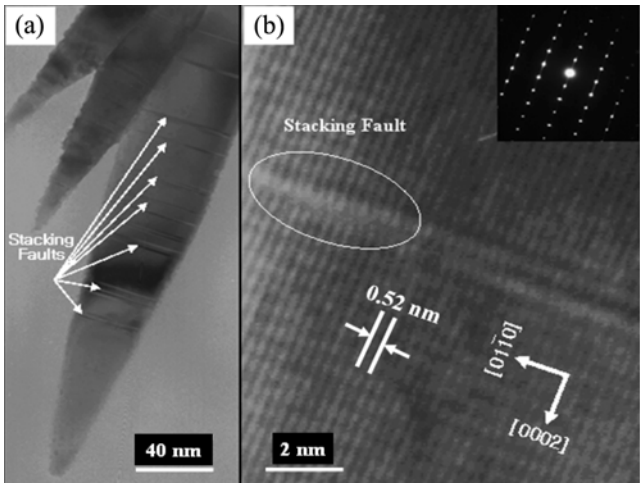

Fig. 4. (a) Low magnification and (b) high resolution TEM (HRTEM) images of ZnO nanoneedles grown on Au-coated Si (100) substrate by the CFCVD system. The corresponding SAED pattern obtained from the single ZnO nanoneedle projected along the [2110] axis (inset (b)).

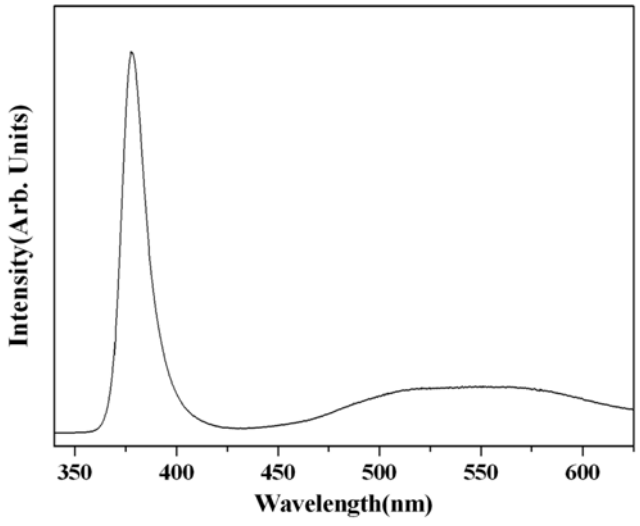

Fig. 5. Room-temperature photoluminescence spectrum of ZnO nanoneedles grown on Au-coated Si(100) substrate measured with the He-Cd laser line with an exciton wavelength of 325 nm.

interstitials etc. in the deposited products. Vanheusden et al. reported that the appearance of green emission in the PL spectrum is due to the recombination of the photogenerated hole with an electron occupying the oxygen vacancies [26]. It is believed that the high crystalline quality ZnO shows a dominant UV emission with a week green emission. Hence, the crystal quality of the deposited ZnO nanostructure has strong influence in the appearance of high UV emission and therefore improvement in the crystal quality (fewer structural defects and impurities such as oxygen vacancies and zinc interstitials) may enhance the intensity of UV emission as compared to the green emission [17,27,28]. Interestingly, by HRTEM observation we found that the as-grown ZnO nanoneedles show some structural defects (i.e., stacking faults) on their surfaces, originating due to the condensation of interstitial Zn atoms which can induce the formation of oxygen vacancies (Fig. 4(b)). Therefore, it gives strong evidence that the green emission in room-temperature PL spectrum of ZnO nanoneedles originates due to the structural defects and is consistent with the PL observation. In our case of ZnO nanoneedles, UV emission dominates over the green emission, which indicates that the grown products have good crystal quality with some structural defects and impurities and are exhibiting good optical properties.

2. Detailed Possible Growth Mechanism of ZnO Nanoneedles

Generally, the conventional vapor-liquid-solid (VLS) mechanism is widely applicable to describe the growth process for various kinds of one-dimensional nanostructures [29,30]. The VLS mechanism consists of the metal particles which act as catalyst for the growth of one-dimensional nanostructures. The process begins from the absorption of a source material from the gas phase into the metal liquid droplets and forms the liquid alloy. When this liquid alloy becomes saturated, a solid precipitate is formed which serves as a preferred site for further deposition. The main characteristic of the VLS mechanism is the presence of metal particles on the tips of the as-grown nanostructures. In our presented results, even a thin layer of gold (10 nm) was coated on Si(100) substrate, but after the deposition no metal catalyst or any type of impurity was detected from the tips of the grown ZnO nanoneedles, as confirmed by the FESEM and TEM observations. Therefore, one can conclude that the growth of ZnO nanoneedles did not follow the VLS mechanism. Fig. 6 shows a possible growth process for the formation of ZnO nanoneedles on Au coated Si(100) substrate. Three steps are assumed to propose a detailed mechanism for the deposited structures, i.e., alloying, nucleation, and growth. After the Au-coated Si(100) substrate was loaded into the reactor chamber (a), the temperature was ramped from room-temperature to the deposition temperature, which provides a sufficient environment for the formation of metal catalyst droplets on the substrate surface. The DEZn, as a source material of Zn, was introduced into the reactor chamber which decomposed into zinc and ethyl vapors. The generated zinc vapors are adsorbed onto the previously formed Au droplets and ethyl vapors are purged out by Ar gas. The adsorbed Zn is then reacted with the introduced oxygen, forms ZnO onto the outer surfaces of Au droplets, and makes the Au/ZnO alloy droplets (b), while the unreacted oxygen is purged out with the introduced argon gas. The formed Au/ZnO alloy droplets may act as a seed and provide nucleation sites for further growth of the final product. After the supersaturation of the Au/ZnO alloy droplets and continuous feeding of the reactants, precipitation of ZnO increases onto the surface of Au/ZnO droplets in [0001] direction. As the concentration of the zinc oxide increases, the thickness of the ZnO over the gold particles increases and gold lies beneath at the base of the formed ZnO nanoneedles (c) [32]. Therefore, no sign of gold particles was observed from the tips of as-grown nanoneedles. Furthermore, the regular supply of diethyl zinc and oxygen gases into the reactor chamber enhances the precipitation on the Au/ZnO nucleation sites and finally needle-shaped ZnO nanostructures are obtained (d). In addition, the ZnO nanoneedles showed sharpened tips with wider bases. It is assumed that the sharpness at their tips originates due to the lack of reactant supply (zinc source and oxygen) to the reactor during the growth of nanostructures. The ZnO is a polar crystal, where zinc and oxygen atoms are arranged alternatively along the c-axis and the top surfaces is Zn-terminated (0001), while the bottom surfaces are oxygen-terminated (000$\bar{1}$). The Zn-(0001) is catalytically active whereas the O-(000$\bar{1}$) is inert [18,31]. Therefore, the {0001} plane is the most rapid growth rate plane while the {000$\bar{1}$} plane has the slowest growth rate. In this case of ZnO nanoneedles, the growth along the [0001] direction is dominant as confirmed by the HRTEM and SAED patterns, and shows consistency with the growth habit of ZnO crystals.

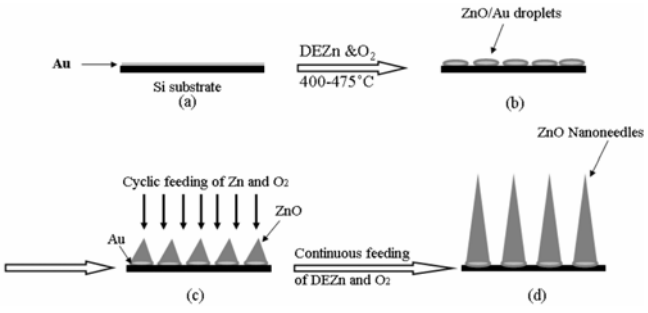

Fig. 6. Schematic illustration of growth mechanism for the needle-shaped ZnO nanostructures grown on Au-coated Si(100) substrate by the cyclic feeding chemical vapor deposition method.

CONCLUSIONS

In summary, ZnO nanoneedles have been successfully grown by the modified CFCVD system on Au-coated Si(100) substrate using the diethyl zinc and oxygen as source materials for zinc and oxygen, respectively. Detailed structural characterizations indicate that the synthesized nanoneedles are single-crystalline with the wurtzite hexagonal phase and grown along the grown along the [0001] direction in preference. The room-temperature PL spectrum exhibits a strong and sharp UV emission with a suppressed and broad green emission, confirmed the good crystallinity and good optical properties for the as-grown products. The deposited ZnO nanoneedles may be applicable for the fabrication of field emission devices, probing tips with high spatial resolution and atomic force microscopy tips etc.

ACKNOWLEDGMENTS

This work was supported by the Brain Korea 21 in 2007 and Korea

Science and Engineering Foundation grant funded by the Korean Government (MOST) (No. R01-2006-000-11306-0).

REFERENCES

1. S. Iijima, *Nature*, **354**, 56 (1991).
2. A. M. Morales and C. M. Lieber, *Science*, **279**, 208 (1998).
3. X. T. Zhang, Z. Liu, Y. P. Leng, Q. Li and S. K. Hark, *Appl. Phys. Lett*., **83**, 5533 (2003).
4. A. Umar, H. W. Ra, J. P. Jeong, E.-K. Suh and Y. B. Hahn, *Korean J. Chem. Eng*., **23**, 499 (2006).
5. A. Sekar, S. H. Kim, A. Umar and Y. B. Hahn, *Journal of Crystal Growth*, **277**, 471 (2005).
6. A. Umar, S. Lee, Y. S. Lee, K. S. Nahm and Y. B. Hahn, *J. Crystal Growth*, **277**, 479 (2005).
7. A. Umar, S. H. Kim, Y. S. Lee, K. S. Nahm and Y. B. Hahn, *J. Crystal Growth*, **282**, 131 (2005).
8. A. Umar, B. Karunagaran, E.-K. Suh and Y. B. Hahn, *Nanotechnology*, **17**, 4072 (2006).
9. (a) S. Lee, Y. H. Im and Y. B. Hahn, *Korean J. Chem. Eng*., **22**, 334 (2005); (b) C. Klingshirn, *Phys. Status Solidi B*, **71**, 547 (1975).
10. S. C. Minne, S. R. Manalis and C. F. Quate, *Appl. Phys. Lett*., **67**, 3918 (1995).
11. B. P. Zhang, N. T. Binh, K. Wakatsuki, Y. Segawa, Y. Yamada, N. Usami and H. Koinuma, *Appl. Phys. Lett*., **84**, 4098 (2004).
12. W. L. Hughes and Z. L. Wang, *Appl. Phys. Lett*., **82**, 2886 (2003).
13. W. L. Hughes and Z. L. Wang, *J. Am. Chem. Soc*., **126**, 6703 (2004).
14. P. X. Gao and Z. L. Wang, *J. Appl. Phys*., **97**, 044304 (2005).
15. X. Y. Kong and Z. L. Wang, *Appl. Phys. Lett*., **84**, 975 (2004).
16. A. Umar, S. Lee, Y. H. Im and Y. B. Hahn, *Nanotechnology*, **16**, 2462 (2005).
17. A. Umar and Y. B. Hahn, *Nanotechnology*, **17**, 2174 (2006).
18. A. Umar and Y. B. Hahn. *Appl. Phys. Lett*., **88**, 173120 (2006).
19. J. L. Yang, S. J. An, W. I. Park, G. C. Yi and W. Choi, *Adv. Mater*., **16**, 1661 (2004).
20. W. I. Park, G. C. Yi, M. Kim and S. J. Pennycook, *Adv. Mater*., **14**, 1841 (2002).
21. Y. B. Li, Y. Bando and D. Golberg, *Appl. Phys. Lett*., **84**, 3603 (2004).
22. H. Z. Zhang, R. M. Wang and Y. W Zhu, *J. Appl. Phys*., **96**, 624 (2004).
23. J. Zhang, Y. Yang, F. Jiang and J. Li, *Physica E*, **27**, 302 (2005).
24. W. A. de Heer, A. Chatelain and D. Ugrate, *Science*, **270**, 1179 (1995).
25. D. Gerthsen, D. Litvinov, Th. Gruber, C. Kirchner and A. Waag, *Appl. Phys. Lett*., **81**, 3972 (2002).
26. K. Vanheusden, C. H. Seager, W. L. Warren, D. R. Tallant and J. A. Voigt, *J. Appl. Phys*., **79**, 7983 (1996).
27. D. M. Bagnall, Y. F. Chen, Z. Zhu, T. Yao, S. Koyama, M. Y. Shen and T. Goto, *Appl. Phys. Lett*., **73**, 1038 (1998).
28. D. M. Bagnall, Y. F. Chen, M. Y. Shen, Z. Zhu, T. Goto and T. Yao, *J. Cryst. Growth*, **185**, 605 (1998).
29. R. S. Wagner and W. C. Ellis, *Appl. Phys. Lett*., **4**, 89 (1964).
30. X. F. Duan and C. M. Lieber, *J. Am. Chem. Soc.*, **122**, 188 (2000).
31. P. X. Gao and Z. L. Wang, *J. Phys. Chem. B*, **108**, 7534 (2004).
32. D. Zhao, C. Andreazza, P. Andreazza, J. Ma, Y. Liu and D. Shen, *Chem. Phys. Lett*., **399**, 522 (2004).